Egyptian Journal of Aquatic Research (2016) 42, 301–312

HOSTED BY

ELSEVIER

National Institute of Oceanography and Fisheries

Egyptian Journal of Aquatic Research

http://ees.elsevier.com/ejar
www.sciencedirect.com

FULL LENGTH ARTICLE

Antibacterial and anticancer activity of extracellular synthesized silver nanoparticles from marine *Streptomyces rochei* MHM13

Hanan M. Abd-Elnaby [a,*], Gehan M. Abo-Elala [a], Usama M. Abdel-Raouf [b], Moaz M. Hamed [a]

[a] *Marine Microbiology Lab., Marine Environ. Div., National Institute of Oceanography and Fisheries, Egypt*
[b] *Microbiology Lab., Faculty of Science, Al-Azhar University – Assuit Branch, Egypt*

Received 12 February 2016; revised 23 May 2016; accepted 29 May 2016
Available online 21 June 2016

KEYWORDS

Silver nanoparticles;
Actinomycetes;
Antibacterial;
Streptomyces rochei MHM13

Abstract The study investigated silver nanoparticles (AgNPs) synthesized extracellularly using an actinomycete isolated from sediment of the Suez Gulf, Red Sea, Egypt. Screening for biosynthesis of AgNPs revealed that among the forty one actinomycetes tested, only two exhibited the ability to synthesize AgNPs with antibacterial activity. The most potent isolate was selected and identified as *Streptomyces rochei* MHM13 (accession number KR108310) on the basis of morphological and physiological properties, together with 16S rRNA sequence. The biosynthesized AgNPs significantly inhibited the growth of medically important pathogenic bacteria (*Vibrio fluvialis*, *Pseudomonas aeruginosa*, *Salmonella typhimurium*, *Vibrio damsela*, *Escherichia coli*, *Bacillus subtilis*, *Staphylococcus aureus*, *Bacillus cereus*). The biosynthesized AgNPs were achieved by addition of silver nitrate (1 mM) to the culture supernatant and monitored by colour change after incubation then characterized by UV–Visible spectrophotometer, X-ray, Fourier transform-infrared spectroscopy and scanning electron microscopy. The obtained AgNPs are spherical in shape with a particle size of 22–85 nm. Plackett–Burman design was employed for optimization of the culture conditions for the production of AgNPs by *S. rochei*. Synergetic effect of AgNPs with six different antibiotics was evaluated. The microbiologically synthesized silver nanoparticles acted as an anti-biofouling agent. Moreover, silver nanoparticles exhibited a significant degree of anticancer activity against five different tumour cell lines.

Introduction

Nanotechnology is a science, dealing with the synthesis of nanoscale materials (range in size from 1 to 100 nm) (Zarina and Nanda, 2014a,b), and their applications. The metallic nanoparticles have various categories including gold, silver,

* Corresponding author at: National Institute of Oceanography and Fisheries (NIOF), Marine Microbiology Lab., Kayet Bay, El-Anfushy, Alexandria, Egypt. Tel.: +20 1005898211; fax: +20 34801553.
E-mail address: hananabdelnaby1@gmail.com (H.M. Abd-Elnaby).
Peer review under responsibility of National Institute of Oceanography and Fisheries.

http://dx.doi.org/10.1016/j.ejar.2016.05.004

alloy, zinc and others (Singh et al., 2014a,b; Bhosale et al., 2015).

Silver nanoparticles have considerable attention among metal nanomaterials, due to their physicochemical properties (Abdeen et al., 2014). They are in great demand due to their widespread applications e.g., antimicrobials and therapeutics, bimolecular detection, biolabeling, catalysis and microelectronics, nonlinear optics and intercalation materials for electrical batteries (Rai et al., 2009; Zarina and Nanda, 2014a; Golinska et al., 2014).

Biological synthesis of metal nanoparticles has been well achieved by different microorganisms (Golinska et al., 2014; Zarina and Nanda, 2014a). Actinomycetes are considered an important resource for new products of medical and industrial interest such as antimicrobial agents (Bhosale et al., 2015; Mohamedin et al., 2015). They are being used as ecofriendly nanofactories (Deepa et al., 2013; Abdeen et al., 2014; Lakhsmi et al., 2015). Actinomycetes are efficient candidates for metal nanoparticles production extracellularly and intracellularly. The synthesis of nanoparticles by actinomycetes represent good stability and polydispersity. Actinomycetes possess important biocidal activity against different pathogens (El-Naggar and Abdelwahed, 2014; Golinska et al., 2014; Mohamedin et al., 2015). Moreover, it can be manipulated genetically in order to provide better control over size (Bhosale et al., 2015).

Optimization of the growth conditions, such as media components, pH, temperature, substrate concentration and inoculum size will not only support the growth but also enhance the productivity and monitor the rate of enzyme activity which affects the synthesis of silver nanoparticles (El-Naggar and Abdelwahed, 2014; Singh et al., 2014b; Iravani, 2014; Mohamedin et al., 2015).

Statistical experimental designs depend on many steps of an optimization strategy, such as searching for optimal conditions of the targeted factor or for screening experiments (Yue et al., 2012; El-Naggar and Abdelwahed, 2014; Mohamedin et al., 2015). Plackett–Burman design is one of the popular and economic choices for bio-processing (Kiran et al., 2010; El-Naggar and Abdelwahed, 2014; Mohamedin et al., 2015).

This study investigates the antibacterial activity and characterization of AgNPs synthesized extracellularly by *Streptomyces rochei* MHM13 isolated from sediment of the Suez Gulf, Red Sea, Egypt. The study extent is to optimize the culture conditions using Plackett–Burman Design. Also, the anticancer activity of silver nanoparticles was assessed.

Materials and methods

Actinomycetes growth conditions

A total of forty one actinomycete isolates representing different colony morphologies were isolated from sediment samples along Suez Gulf, Red Sea, Egypt, during February, 2015. Actinomycetes were cultivated on starch-nitrate medium (Abou-Elela et al., 2009) with the following components ($g\ l^{-1}$): 20 starch, 0.5 K_2HPO_4, 1 KNO_3, 0.5 $MgSO_4{\cdot}7H_2O$, 0.01 $FeSO_4$, 15 agar (for solid medium), pH 7 and incubation was performed at 30–32 °C for seven days.

Pathogenic indicators

The bacterial pathogens were *Bacillus subtilis* 6633, *Staphylococcus aureus* 25,923, *Pseudomonas aeruginosa* 9027, *Bacillus cereus*, *Salmonella typhimurium* 14,028, *Escherichia coli* 19,404, *Vibrio fluvialis* and *Vibrio damsela*.

Preparation of cell free extract

Each isolate from the forty one actinomycetes was inoculated in 250 ml flask containing starch-nitrate medium (50 ml). Inoculated flasks were incubated in a rotary shaker at 200 rpm and 30–32 °C for seven days. After incubation, each culture was centrifuged at 12,000 rpm and its supernatant was used for further experiments (Selvakumar et al., 2012).

Biosynthesis of silver nanoparticles (AgNPs)

Aqueous solution of 1 mM silver nitrate (50 ml) was mixed with actinomycete supernatants (50 ml) and the pH was adjusted to 8.5. The mixture was incubated in a rotary shaker at 37 °C and 200 rpm in the dark for 5 days. Control experiments were performed with un-inoculated media and silver nitrate solution to check the role of bacteria in the nanoparticle synthesis. The silver ions reduction was examined by sampling about 2 ml of the solution at time intervals and monitoring the UV–Vis spectra by using UV–Vis spectrophotometer (Double Beam Spectrophotometer 6800 JENWAY). In each reaction vessel colour change was observed to yellowish brown in the silver nitrate solution incubated with actinomycetes supernatant (Selvakumar et al., 2012).

Antibacterial assay

The antagonistic activity of the biosynthesized AgNPs was tested by well-cut diffusion technique, in which, wells (5-mm) were punched in Muller Hinton agar (Oxoid Ltd, England) plates inoculated with pathogenic bacteria. Fifty microlitres of AgNPs were pipetted into each well. After incubation at 37 °C overnight, the radius of the inhibition zone around each well was measured in mm (Priyaragini et al., 2013). This test was done in duplicate.

Identification of the most potent isolate

Genotypic characterization

DNA of the selected actinomycetes isolate was extracted and purified. The region of 16S rDNA was amplified using either species specific primers or universal primers. Genotypic characterization was carried out by using 16S sequence analysis. Finally, the multiple alignments with sequences of most closely related members and the levels of sequence similarity were performed using Bioedit (Hall, 1999). For comparison, Sequences of rRNA genes were detected from the database of NCBI.

Phenotypic characterization

The morphological, cultural, physiological, biochemical characteristics for the selected actinomycete isolate were performed according to standard procedure of Bergey's Manual of Determinative Bacteriology (Ravikumar and Krishnakumar, 2010).

Electron microscopy study

The selected actinomycetes' isolate was cultured in starch nitrate agar medium and incubated at 30–32 °C for 14 days. A specimen of the culture was fixed in glutaraldehyde (2.5%, v/v), and washed by water, then, post-fixed in 1%, w/v osmium tetroxide for one hour. The sample was washed with water (twice) and dehydrated by ascending concentrations of ethanol (30–100%, v/v). The sample was coated by gold and examined at 15–20 kV by scanning electron microscope (JEOL JSM 5400 LV), Japan, at the electron microscope unit of Assiut University, Egypt.

Confirmation for the presence of extracellular silver nanoparticles

UV–Visible spectroscopy (UV–Vis)

The bioreduction of silver ions was monitored by colour change from pale yellow to brown. Further, it was confirmed by sharp peaks observed by the absorption spectrum of this solution by using UV–Vis spectrophotometer (Double Beam Spectrophotometer 6800 JENWAY). An aliquot of the tested solution was taken in a cuvette (quartz) and monitored for wavelength scanning from 300 to 700 nm (Singh et al., 2014a).

Energy dispersive X-ray analysis (EDX)

Elemental analysis energy dispersive, X-ray analysis (EDX) was done using X-ray microanalysis system coupled with scanning electron microscope (SEM) (El-Agamy, 2014). It was carried out at the Center of Biotechnology and Mycology, El-Azhar University, Cairo, Egypt.

Fourier transform infrared spectroscopy (FT-IR)

For Fourier transform infra-red (FT-IR) spectroscopy measurements, the bio-transformed products found in the extracellular supernatant from *S. rochei* MHM13 were freeze dried then diluted by potassium bromide (the ratio 1:100). The FT-IR spectrum of the sample was monitored on FT-IR instrument attached with diffuse reflectance mode (DRS-800). All measurements were performed in the range from 400 to 4000 cm^{-1} at a resolution of 4 cm^{-1}. To identify the functional groups found in the tested sample, the spectral data recorded were compared with the reference chart (Deepa et al., 2013). It was carried out at the Center of Biotechnology and Mycology, El-Azhar University; Cairo, Egypt.

Scanning electron microscopy (SEM)

SEM was carried out to observe the morphology, shape and size of the produced nanoparticles. A specimen was performed by casting a drop of the mixture on a carbon-coated copper grid then, the excess solution was removed and allowed to dry in the air. The study of scanning electron microscopy was monitored on S-3400 2010 (Japan) at an accelerating voltage of 10,000 V (attached with a CCD camera) (Kumar et al., 2015).

Application of Plackett–Burman design for optimization of the culture conditions

The Plackett–Burman experimental design was applied to evaluate the relative importance of various factors (Plackett and Burman, 1946) involved in the production of silver nanoparticles by *S. rochei* MHM13 and its antibacterial activity against *V. fluvialis*. The seven independent variables tested in this application and their settings are recorded in Table 1. Each variable was examined in four trials at high level (+1) and in four trials at low level (−1). The eight different trials and the basal control were performed in duplicate. The main effect for each variable was measured with the following equation:

$$\mathrm{Exi} = \left(\sum \mathrm{M_{i+}} - \sum \mathrm{M_{i-}}\right)/\mathrm{N}$$

where Exi is the main effect variable, M_{i+} and M_{i-} are the radius (mm) of the inhibition zone around each well. Also, the independent variable (xi) was present in low and high concentrations, respectively, while, N represented the number of trials divided by 2. The statistical *t*-values for equal unpaired samples were calculated using Microsoft Excel to measure the variable significance (Cochran and Snedecor, 1989). An optimized medium was predicted from the main effect results.

Verification experiment

The predicted optimum levels for the independent variables were carried out and compared with the basal conditions and the averages of inhibition zones were calculated. This experiment was performed in duplicates.

Silver nanoparticles and their antibiotic efficacy

The antimicrobial activity of the biosynthesized AgNPs was examined against bacterial pathogens. The combined formulation of silver nanoparticles with standard antibiotic discs selected from different groups having a different mode of action includes: Ciprofloxacin (CIP, 5 µg/disc; fluoroquinolones group), Ampicillin (AM, 10 µg/disc; betalactam antibiotics group), Streptomycin (S, 10 µg/disc), Gentamicin (GN, 10 µg/disc; aminoglycoside), Tetracycline (TE, 10 µg/disc; ulphoamides group), and Lincomycin (L, 2 µg/disc). They were used to find out the synergistic effect against the tested bacterial pathogens. After incubation overnight at 37 °C, the inhibition zone (mm) was measured (Zarina and Nanda, 2014a). The increase in fold area was estimated by measuring the mean surface area of the clear inhibition zone produced by an antibiotic alone and in combination with silver nanoparticles, (Fayaz et al., 2010; Zarina and Nanda, 2014a).

Table 1 Independent variables affecting antibacterial activity of silver nanoparticles.

Factor	Symbol	Level		
		−1	0	+1
Starch ($g\ l^{-1}$)	Starch	10	20	30
KNO_3 ($g\ l^{-1}$)	KN	0.5	1.0	1.5
K_2HPO_4 ($g\ l^{-1}$)	K_2	0.25	0.5	0.75
$MgSO_4{\cdot}7H_2O$ ($g\ l^{-1}$)	Mg	0.25	0.5	0.75
$FeSO_4$($g\ l^{-1}$)	Fe	0.005	0.01	0.015
Temperature (°C)	Temp	33	35	37
pH	pH	6.5	7.5	8.5

*Inoculum size was added as 1 ml of 7 days culture (10^3 CFU ml^{-1}).

Antifouling activity

Seawater (1 ml) was mixed with nutrient broth medium (20 ml) (Oxoid Ltd, England) in conical flask (50 ml) containing cover glass and incubated overnight at 28 °C. About 200 µl of silver nanoparticles was added into the flask (as an antifouling agent). After dying with crystal violet solution (0.4%) for ten minutes, the cover glass was washed by water, dried at room temperature and observed under the microscope (Kumaran et al., 2011). For comparison, a control flask without silver nanoparticles was used.

Anticancer activity

To evaluate the anticancer activity of AgNPs produced by *S. rochei* HMM13, several steps were carried out: lyophilization, cytotoxicity test (measured by MTT assay) and effect of the median inhibitory dose (IC_{50}) (Abd-Elnaby et al., 2016; El-Sersy et al., 2012) on eight different tumour cell lines: Hepatocellular carcinoma cells (HepG-2), Breast carcinoma cells (MCF-7), Colon carcinoma cells (HCT-116), Prostate carcinoma cells (PC-3), Lung carcinoma cells (A-549), Intestinal carcinoma cells (CACO), Larynx carcinoma cells (HEP-2) and Cervical carcinoma cells (HELA).

Results and discussion

Screening for biosynthesis of silver nanoparticles

The current study was focused on the extracellular synthesis of AgNPs by actinomycete supernatant. A total of forty one actinomycetes were checked for their ability to produce silver nanoparticles. The screening revealed that only two isolates; 13 and 38 showed the ability to synthesis AgNPs. The Erlenmeyer flasks with the actinomycetes supernatant was pale-yellow in colour before the addition of silver ions and this colour changed to yellowish-brown at the end of the reaction with silver ions (Fig. 1).

The yellowish-brown colour that appeared in the flasks mixed with silver nitrate was a clear indication of silver nanoparticle formation (Sastry et al., 2003) due to the reduction of Ag^+ ions and formation of surface plasmon resonance in the reaction mixture, while no colour change appeared in culture filtrates without silver nitrate (Narasimha et al., 2013; Zarina and Nanda, 2014a). The synthesis of nanoparticles by actinomycetes has many advantages e.g. they are safe to handle, easily available, and possess variable metabolites that may help in reduction. Moreover, these particles have innumerable applications (Deepa et al., 2013).

Antibacterial activity of silver nanoparticles

The microbiologically synthesized AgNPs exhibited an excellent antibacterial activity against the bacterial pathogens both gram negative and gram positive (Table 2). Silver nanoparticles synthesized by actinomycete isolate 13 exhibited the maximum zones of inhibition (16–19 mm) against all tested pathogenic bacteria, whereas, silver nanoparticles synthesized by actinomycete isolate 38 exhibited moderate zones of inhibition (13–18 mm) against some tested pathogenic bacteria and failed to inhibit two pathogens (Fig. 2). Generally, silver nanoparticles produced by actinomycete isolate 13 showed higher activity against the tested pathogens, and exhibited the strong action against *V. fluvialis*, so it's selected for further studies.

The formation of inhibition zone around the well was an indication of antibacterial activity of silver nanoparticles (Narasimha et al., 2013). Silver nanoparticles exhibited a broad bactericidal activity against gram positive and gram

Table 2 Inhibition zone (mm) of the silver nanoparticles (50 µl) synthesized by isolates 13 and 38 against some bacterial pathogens.

Pathogenic bacteria	Isolate 13	Isolate 38
	AgNPs inhibition zone (mm)	
Bacillus subtilis	18	16
Staphylococcus aureus	18	18
Pseudomonas aeruginosa	18	0
Bacillus cereus	16	14
Salmonella typhimurium	18	14
Escherichia coli	16	0
Vibrio fluvialis	19	15
Vibrio damsela	16	13

Isolate 13 **Isolate 38**

Figure 1 The supernatant of actinomycetes isolates (13 and 38) were mixed with 1 mM $AgNO_3$ at the beginning of incubation (a pale yellow colour) and after 72 h of incubation (a yellowish-brown colour).

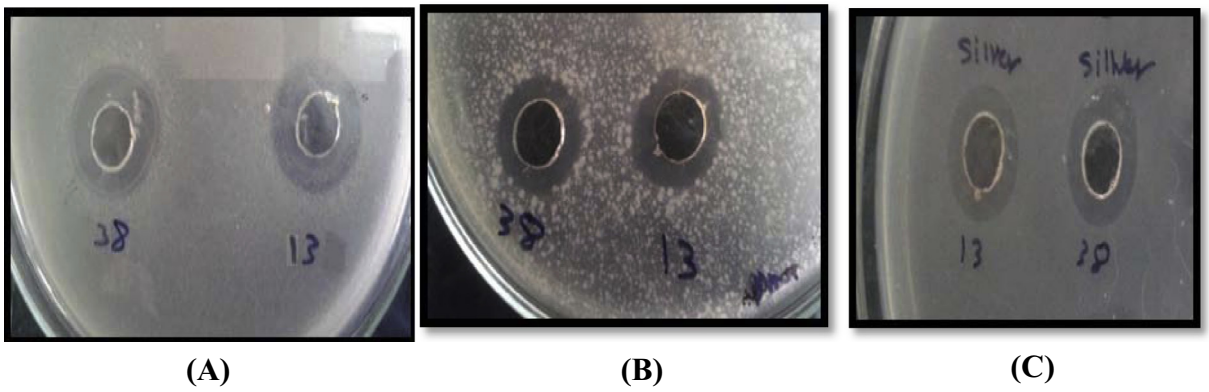

Figure 2 Antagonistic effects of AgNPs synthesized by actinomycetes isolates 13 and 38 against (A): *Vibrio fluvialis* (B): *Staphylococcus aureus* and (C): *Bacillus subtilis*.

negative bacteria as well as multiresistant strains (Shrivastava et al., 2007). Similarly, Jaidev and Narasimha (2010), Narasimha et al. (2013) and Kamel et al. (2016) demonstrated the reactive antimicrobial activity of silver nanoparticles. Also, Saminathan (2015) showed that silver nanoparticles synthesized by *Streptomyces* sp. have reactive antibacterial activity against test pathogens including *S. aureus*, *Proteus vulgaris*, *E. coli*, *Shiegella dysentriae*, *Klebsiella pneumonia* and *Salmonella typhi*.

Identification of the most potent isolate

The most potent actinomycete (isolate 13) that produced silver nanoparticles capable of inhibiting the growth of all tested pathogenic bacteria was selected. This actinomycete was identified by phenotypic characterization and molecular phylogenetic analysis.

Genomic DNA of actinomycetes 13 was extracted, and the 16S rDNA gene was partially amplified. The produced amplicons of the selected isolate was detected using agarose gel electrophoresis. The sequence obtained from 16S rRNA gene showed that the actinomycete isolate was similar to *S. rochei* with an identity of 99%. The sequence of nucleotide was deposited to the database of GenBank as *S. rochei* MHM13 with accession number KR108310. Fig. 3 represents the phylogenetic relationships between representative experimental strains and the most closely related species. Some morphology, cultural and biochemical characteristics of *S. rochei* MHM13 were studied and represented in Table 3. Also, Fig. 4 represents the spore formation of *S. rochei* MHM13.

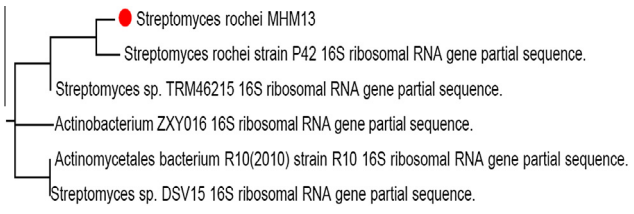

Figure 3 Phylogenetic analysis of *Streptomyces rochei* MHM13 based on partial sequencing of 16S rDNA.

Table 3 Phenotypic characteristics of *Streptomyces rochei* MHM13.

Test		Test	
Diffusible pigments	Beige	Urea hydrolysis	+
Aerial mycelium	Grey	Gelatin hydrolysis	+
Substrate mycelium	Yellow	Protease production	+
Growth on		H_2S production	–
Starch nitrate agar	+	Methyl red	+
Inorganic salts starch agar	+	Voges proskauer	–
Krassilnikov agar	+	Indole	–
Glycerol-nitrate agar	+	Nitrate reduction	+
Glucose yeast-malt extract agar	–	Citrate	+
Cazpex Dox agar	+	Catalase	+
Oat meal agar	+	Starch	+
Growth at (°C)		Aesculin	+
25–30	+	Arginine dihydrolase	+
40–50	–		

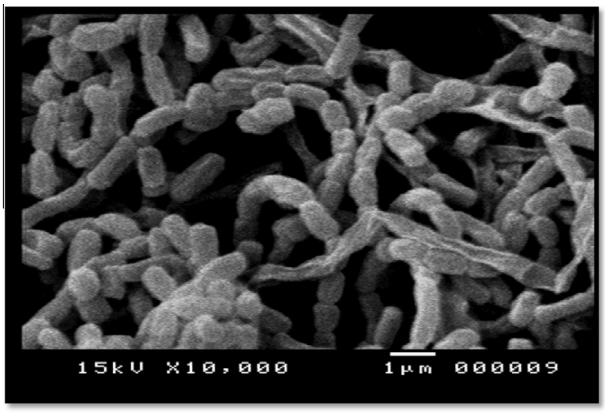

Figure 4 Scanning electron micrograph shows spore formation of *Streptomyces rochei* MHM13 after 14 days of incubation on starch-nitrate agar medium.

Several studies reported the potential of *Streptomyces* sp. in biosynthesized of silver nanoparticles (Samundeeswari et al., 2012; Chauhan et al., 2013; Prakasham et al., 2014; Singh

et al., 2014a; Zarina and Nanda, 2014a,b; Saminathan, 2015). Selvakumar et al., (2012) mentioned that AgNPs have been successfully synthesized by marine *S. rochei*. Also, Reddy et al. (2011) investigated the characterization *of S. rochei*.

Characterization of silver nanoparticles synthesized by S. rochei MHM13

UV–Visible spectroscopy

The absorption spectrum of the AgNPs synthesized by *S. rochei* is illustrated in Fig. 5. The absorption obtained indicated a strong surface plasmon resonance band maximum at 410 nm, a characteristic peak for silver nanoparticles. The absorbance peak reflects the size and shape of $AgNO_3$ (Sosa et al., 2003). The surface plasmon resonance peak shifts to longer wavelengths with increase in particle size (Brause et al., 2002). Samundeeswari et al. (2012) mentioned that the extracellular synthesized silver nanoparticles by *Streptomyces albogriseolus* were characterized by an ultraviolet visible spectrophotometer and the maximum absorption spectra was observed at 409 nm. Similar results were showed by Narasimha et al. (2013) and Zarina and Nanda (2014a).

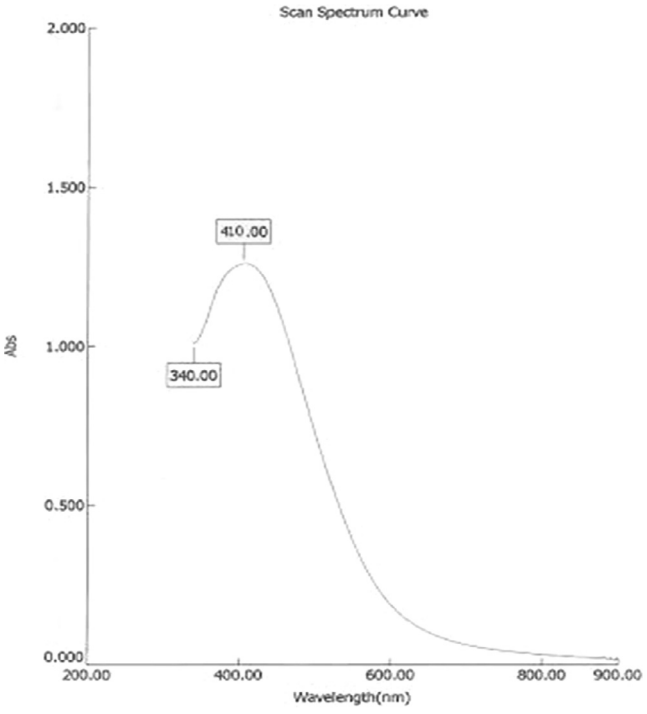

Figure 5 UV–Vis absorption spectrum of AgNPs synthesized by *Streptomyces rochei* MHM13 (treating by 1 mM $AgNO_3$ solution with actinobacteria supernatant).

Energy dispersive X-ray analysis (EDX)

The result of X-ray microanalysis of the silver peck in AgNPs synthesized by *S. rochei* is represented in Fig. 6 which showed the optical absorption peak at 3.5 keV, typical of absorption of metallic silver nanoparticles. Silver nanoparticles have been characterized using X-ray microanalysis (Shaligram et al., 2009; Mohamedin et al., 2015).

Fourier transform infrared spectroscopy

The FT-IR gives insights about the presence of functional groups in the synthesized silver nanoparticles in order to understand how they transform from simple inorganic silver nitrate to elemental silver due to the effect of different photochemicals that might act in a simultaneous way as reducing, stabilizing and capping agent. The spectrum of FTIR evidently shows the bio fabrication of silver nanoparticles mediated by *S. rochei* MHM13 at array of absorbance bands from 400 to 4000 cm^{-1}. The FT-IR spectrum analysis for AgNPs represented intense absorption bands at 3420.14, 2932.23, 2362.37, 1639.20, 1430.92, 1115.62 and 613.252 cm^{-1}, respectively. The intense medium absorbance peak at 3420.14 cm^{-1} (N–H stretch) was characteristic of the amine group (Fig. 7, Table 4). Similar results were reported by Zarina and Nanda (2014a,b), Singh et al. (2014a), Prakasham et al. (2014) and Lakhsmi et al. (2015). The studies of FT-IR confirmed the fact that amide groups of proteins have a stronger ability to bind metal which indicates that the proteins act as capping agent for stabilizing the nanoparticles (Zayed et al., 2012).

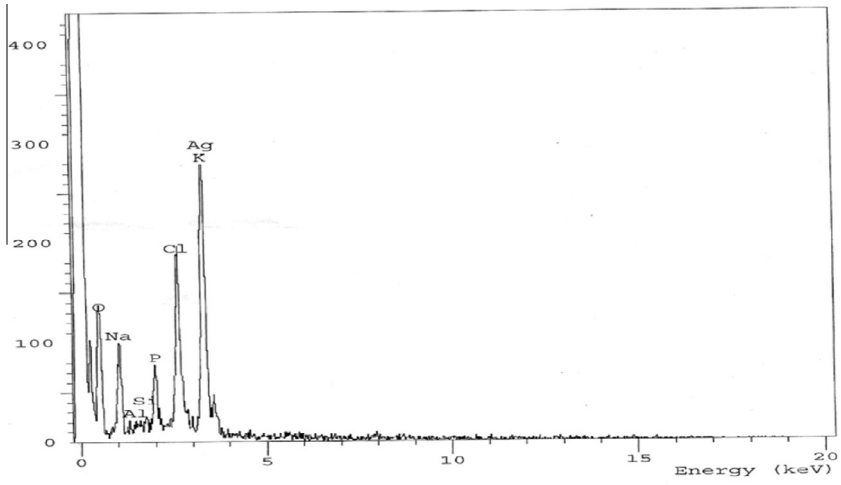

Figure 6 X-ray microanalysis of AgNPs synthesized by *Streptomyces rochei* MHM13 with silver peak at 3.5 keV.

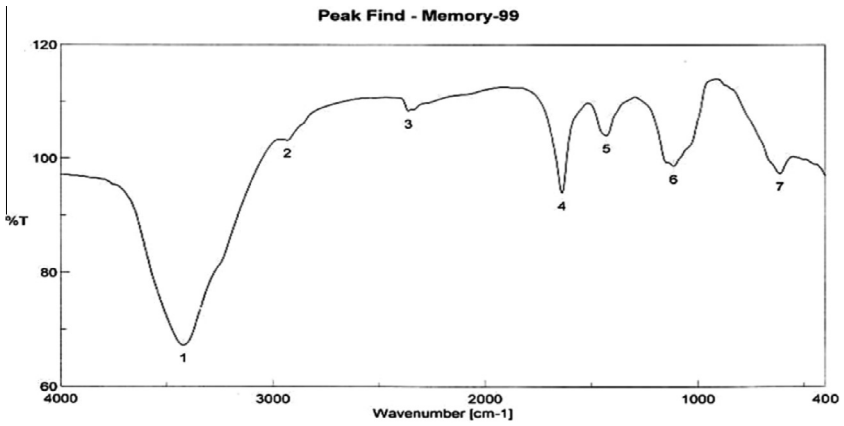

Figure 7 FT-IR analysis of AgNPs synthesized by *Streptomyces rochei* MHM13.

Table 4 FT-IR analysis of AgNPs synthesized by *Streptomyces rochei* MHM13.

Peak No.	Group frequency (cm^{-1})	Functional group assignment
1	3420.14	N—H (stretch primary amine)
2	2932.23	C—H (stretch alkane)
3	2362.37	O═C═O (stretch carbon dioxide)
4	1639.20	C═C (stretch alkene)
5	1430.92	C—H (bend alkane)
6	1115.62	C—O (stretch aliphatic ether)
7	613.252	C—Cl or C—Br (stretch halo compounds)

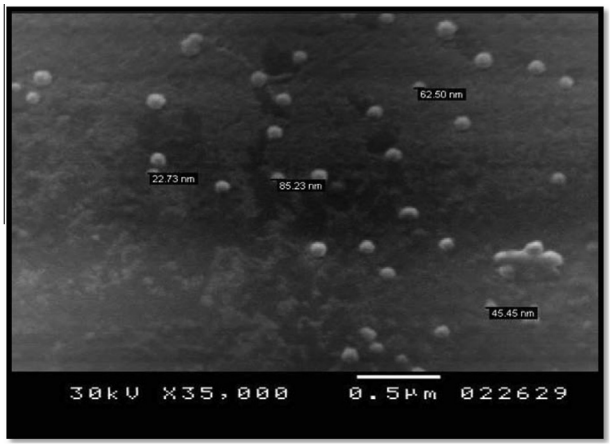

Figure 8 SEM analysis of AgNPs synthesized by *Streptomyces rochei* MHM13.

Scanning electron microscopy

The scanning electron microscope analysis was carried out to depict the shape and size of the silver nanoparticles synthesized by *S. rochei* MHM13. The SEM shows that the bacterium has tremendous capability to synthesize silver nanoparticles which were well defined separated as much as possible, spherical in shape. The obtained nanoparticles were in the size ranging from 22 to 85 nm (Fig. 8). Deepa et al. (2013) reported that silver nanoparticles synthesized from marine *Actinomycetes* shows size of nanoparticles ranging from 20 to 30 nm. Saminathan (2015) showed that the average size of biosynthesized silver nanoparticles were greater than 50 nm and spherical in shape. While Bhosale et al. (2015) found that the biosynthesized silver nanoparticles were irregular in shape. Also, Devika et al. (2012) mentioned that the spherical nanoparticles have diameter that ranged from 40 to 50 nm. Faghri and Salouti (2011) found that the extracellular biosynthesized silver nanoparticles were spherical and the size ranged from 10 to100 nm.

Optimization of the culture conditions by application of Plackett–Burman design

This design has been applied to evaluate the significant effect of starch nitrate medium components for production of AgNPs by *S. rochei* MHM13 and its antibacterial activity against *V. fluvialis*. The starch nitrate medium components and other cultural factors such as pH and temperature were tested according to a design matrix (Table 5) with respect to the AgNPs production and its effect against the fish pathogen *V. fluvialis*.

Table 5 The experimental results of Plackett–Burman design for seven variables affecting antibacterial activity of AgNPs against *Vibrio fluvialis*.

Trials	Starch	KN	K_2	Mg	Fe	Temp	pH	Inhibition zone (mm)
1	–	+	+	+	–	–	–	18
2	+	+	–	–	–	–	+	26
3	+	–	+	–	–	+	–	16
4	–	–	–	+	–	+	+	22
5	+	–	–	+	+	–	–	18
6	–	–	+	–	+	–	+	25
7	–	+	–	–	+	+	–	22
8	+	+	+	+	+	+	+	0
9	0	0	0	0	0	0	0	20

The main effects of each variable on the diameters of inhibition zones were calculated and the *t*-values were estimated for each variable to identify the statistical significance of the measured response and determine the main effects for *S. rochei* MHM13 (Table 6). Based on the present results, the low level

Table 6 Statistical analyses of the Plackett–Burman experimental results.

Variable	Main effect	*t*-value*
Starch	−0.25	2.353
KNO_3	**−6.75**	2.131
K_2HPO_4	−4.25	2.131
$MgSO_4{\cdot}7H_2O$	**−7.75**	2.131
$FeSO_4$	**−7.75**	2.131
Temperature	**−6.75**	2.353
pH	−3.75	2.131

t-value, significant at 5% level = 2.446.
t-value, significant at 10% level = 1.94.
t-value, significant at 20% level = 1.372.
Standard *t*-values are obtained from Statistical Methods by Cochran and Snedecor (1989).
* *t*-value, significant at 1% level = 3.70.

of all variables in the culture medium can increase the suppression of bacterial pathogen (*V. fluvialis*) with respect to production of the of silver nanoparticles by *S. rochei* MHM13 (Fig. 9).

Verification experiment

This experiment was carried out to verify the optimization conditions to validate the obtained optimized medium. *S. rochei* was grown on the optimized medium of the following components ($g\,l^{-1}$): 10 starch, 0.5 KNO_3, 0.25 K_2HPO_4, 0.25 $MgSO_4{\cdot}7H_2O$, 0.005 $FeSO_4$, at pH 6.5 and 33 °C, recorded the larger inhibition zone (24 mm) than that in the basal conditions by 1.26 fold increase. The present result confirmed the validity of the optimized conditions (Fig. 10). The size of AgNPs synthesized by *S. rochei* MHM13 after growth on optimized conditions decreased to the range from 18 to 27 nm (Fig. 11). The smaller silver nanoparticles showed stronger antibacterial activity (Abdeen et al., 2014).

Mohamedin et al. (2015) found that among the fourteen variables tested, peptone concentration medium volume and inoculum age were the most significant factors for silver nanoparticles production from *Streptomyces viridodiastaticus*. Singh et al. (2014b) reported that, the maximum AgNPs production was achieved at 25 °C while at high temperature (40 °C) the enzyme activity decreased so the synthesis of AgNPs slows down in the reaction. On the other hand, the internal environment of living cells is believed to be nearly neutral, so the activity of bacteria decreased as the pH deviates

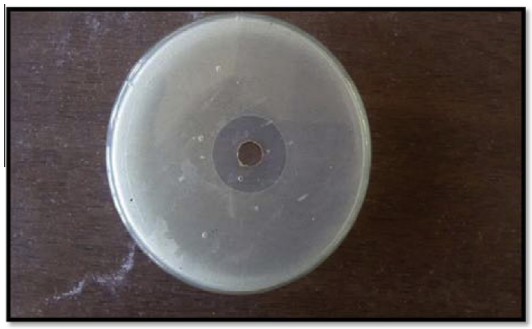

Figure 10 Activity of AgNPs synthesized by *Streptomyces rochei* MHM13 against *Vibrio fluvialis* grown on optimized medium.

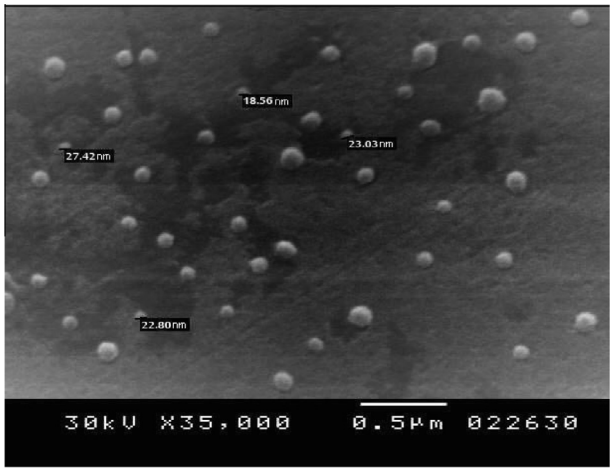

Figure 11 SEM analysis of AgNPs synthesized by *Streptomyces rochei* MHM13 after growth on optimized medium.

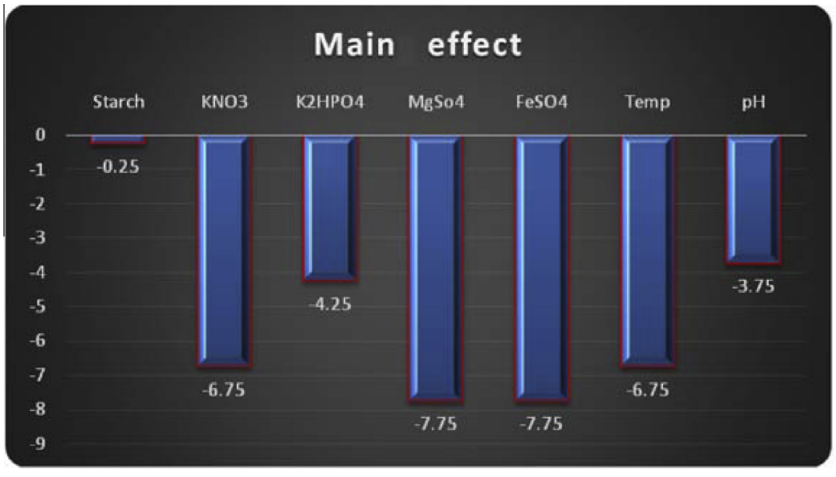

Figure 9 Main effect of the different factors influencing the AgNPs synthesized by *Streptomyces rochei* MHM13.

Table 7 Synergistic effect of antibiotics with and without silver nanoparticles against different pathogenic bacteria.

Pathogenic bacteria	Antibiotic	Inhibition zone (mm)	
		Ab*	Ab + AgNPs**
Vibrio fluvialis	Ciprofloxacin	20	22
	Ampicillin	–	15
	Streptomycin	–	22
	Gentamicin	8	20
	Tetracycline	–	10
	Lincomycin	–	18
Vibrio damsela	Ciprofloxacin	20	30
	Ampicillin	20	25
	Streptomycin	10	25
	Gentamicin	20	25
	Tetracycline	–	25
	Lincomycin	–	20
Salmonella typhimurium	Ciprofloxacin	12	25
	Ampicillin	–	15
	Streptomycin	–	18
	Gentamicin	4	25
	Tetracycline	–	8
	Lincomycin	–	20
Escherichia coli	Ciprofloxacin	18	20
	Ampicillin	–	15
	Streptomycin	–	18
	Gentamicin	12	20
	Tetracycline	–	12
	Lincomycin	–	22

* Ab = antibiotic alone.
** Ab + AgNPs = antibiotic with silver nanoparticles.

from neutral conditions (Malarkodi et al., 2013; El-Naggar and Abdelwahed, 2014; Mohamedin et al., 2015).

Synergetic effect of silver nanoparticles with antibiotics

The various bacterial pathogens exhibited different susceptibilities to AgNPs. The combined effect of AgNPs with six standard antibiotic discs (Ciprofloxacin, Ampicillin, Streptomycin, Gentamicin, Tetracycline and Lincomycin) was observed against some multi drug resistant pathogenic bacteria. The inhibition zones diameters for antibiotics alone and in combination with AgNPs developed significant increase in the fold area for all tested cases (Table 7). The antibacterial activity of the tested antibiotics increased in the presence of AgNPs against test bacterial pathogens (Fig. 12). Similar results were observed by previous studies (Fayaz et al., 2010; Zarina and Nanda, 2014a,b). The combination of AgNPs with antibiotics has better antimicrobial effects. This combination would prevent a development of resistance by pathogenic microbes and also enhance the antimicrobial properties of the antibiotics, moreover, would also decrease the dosage of antibiotic against multi-drugs resistance pathogenic microbes.

Anti-fouling activity of silver nanoparticles

The inhibitory activity of *S. rochei* HMM13 silver nanoparticles on bacterial biofilm formation is illustrated in Fig. 13. The AgNPs reduced the density of bacterial cells and acted as an anti-biofouling agent. The present result agreed with

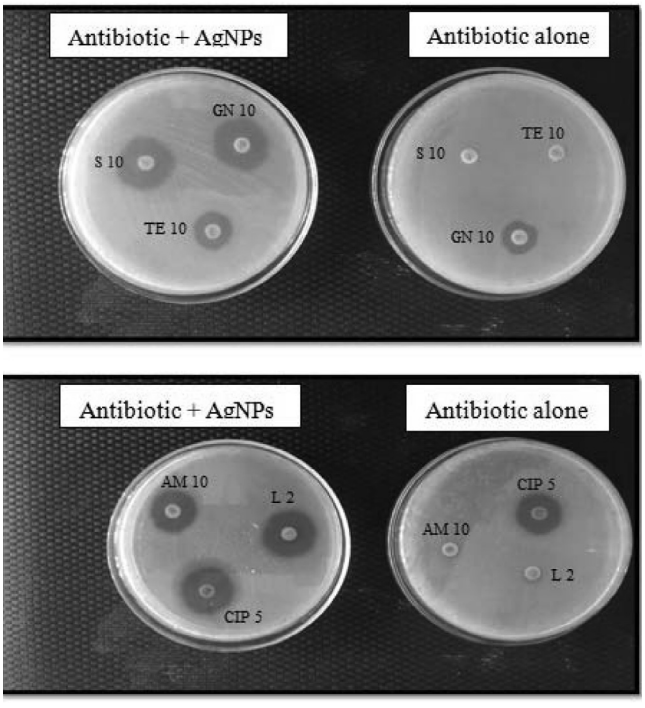

Figure 12 Synergistic effect of various antibiotics with and without AgNPs against *Vibrio fluvialis*.

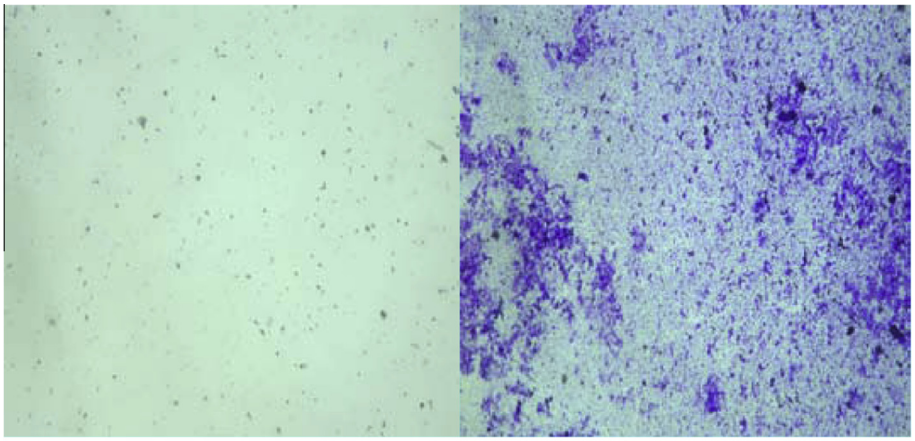

Figure 13 Photographs illustrating the antifouling effect of the AgNPs from *S. rochei* HMM13 on the biofilm formation (A) and the effect without the silver nanoparticles (B).

Table 8 IC_{50} determination cell viability was measured by MTT assays on different cancer cell lines after 24 h exposure to doses of AgNPs produced by *S. rochei* HMM13.

Cell line	IC_{50} (μg/Well)
HepG2	32.90
HCT-116	9.05
MCF-7	40.00
PC-3	48.50
A-549	42.10
CACO	> 50
HEP-2	> 50
HELA	> 50

the study of Sawada et al. (2012) on membrane containing AgNPs with both antibacterial properties and organic antifouling. The study explained that, more than 99.9% of *E. coli* cells were inhibited, suggesting that, the AgNPs were useful for inhibiting bacterial growth.

Anticancer activity of silver nanoparticles

As clearly shown in Tables 8 and 9, the effect of silver nanoparticles on a tumour cell line showed a dose-dependent decrease in viability percentage of cell lines. Silver nanoparticles from *S. rochei* HMM13 exhibited a reasonable degree of anticancer activity after a 24 h exposure to different concentrations of AgNPs, where Hep-G2, HCT-116, A-549 and MCF-7, PC-3 cell lines were the most sensitive cell lines towards the cytotoxic activity of the tested AgNPs, while the CACO, HEP-2, HELA cell lines were the most resistant cell lines towards the cytotoxic activity. In similar results, Kaler et al. (2013) reported that silver nanoparticles at very low concentration showed very high activity on MCF-7 cells, showing almost 80% inhibition. At higher concentration (10–100 μg/mL) no significant difference in inhibition of cancer cells was observed with silver nanoparticles and the IC_{50} value for the silver nanoparticles was less than 10 μg/ml. Also, Shawkey et al. (2013) found that the HCT-116 and Hep-G2 cell lines were the most sensitive cell lines towards the cytotoxic activity of AgNPs, while the Caco-2 cell line was the most resistant cell line towards cytotoxic activity.

Conclusion

A crucial need in the field of nanotechnology is the development of eco-friendly and reliable process for nanoparticles synthesis. It is thus concluded from this study that the marine

Table 9 Anticancer activity for different concentrations of AgNPs which produced by *S. rochei* HMM13 against different cancer cell lines (measured by MTT assays after 24 h exposure).

AgNPs conc. (μg/Well)	HepG-2	MCF-7	HCT-116	PC-3	A-549	CACO	HEP-2	HELA
	Viability%							
50.00	21.63	36.42	17.97	48.13	38.59	54.31	63.82	56.79
25.00	63.14	70.31	24.85	79.24	74.62	78.29	85.17	74.13
12.50	78.92	84.19	37.28	91.36	87.31	91.45	94.26	85.82
6.25	89.56	89.27	60.35	98.63	94.05	98.73	99.02	92.45
3.13	94.32	94.53	83.51	100.00	98.79	100.00	100.00	98.37
1.56	98.75	97.46	91.84	100.00	100.00	100.00	100.00	100.00
0.00	100.00	100.00	100.00	100.00	100.00	100.00	100.00	100.00

Hepatocellular carcinoma cells (HepG-2), breast carcinoma cells (MCF-7), colon carcinoma cells (HCT-116), prostate carcinoma cells (PC-3), lung carcinoma cells (A-549), intestinal carcinoma cells (CACO), larynx carcinoma cells (HEP-2) and cervical carcinoma cells (HELA).

S. rochei HMM13 has been used efficiently for AgNPs' synthesis. We have described the use of low cost, natural and renewable bio-reducing agent. It was confirmed that AgNPs can be bio-synthesized by UV–Visible spectroscopy, EDX, FT-IR and SEM. Optimization of the culture conditions for *S. rochei* HMM13 decreased the size of synthesized AgNPs to the range from 18 to 27 nm. The biosynthesized AgNPs using *S. rochei* HMM13 showed good antibacterial, antifouling and anticancer activity.

Conflicts of interest

The authors declare that there are no conflicts of interest.

References

Abdeen, S., Geo, S., Sukanya, S., Praseetha, P.K., Dhanya, R.P., 2014. Biosynthesis of Silver nanoparticles from *Actinomycetes* for therapeutic applications. Int. J. Nano Dimension 5 (2), 155–162.

Abd-Elnaby, H., Abo-Elala, G., Abdel-Raouf, U., Abdelwahab, A., Hamed, M., 2016. Antibacterial and anticancer activity of marine *Streptomyces parvus*: optimization and application. Biotechnol. Biotechnol. Equip. 30 (1), 180–191.

Abou-Elela, G.M., El-Sersy, N.A., Wefky, S.H., 2009. Statistical optimization of cold adapted á-amylase production by free and immobilized cells of *Nocardiopsis aegyptia*. J. Appl. Sci. Res. 5 (3), 286–292.

Bhosale, R.S., Hajare, K.Y., Mulay, B., Mujumdar, S., Kothawade, M., 2015. Biosynthesis, characterization and study of antimicrobial effect of silver nanoparticles by *Actinomycetes* spp. Int. J. Curr. Microbiol. Appl. Sci. 2, 144–151.

Brause, R., Moeltgen, H., Kleinermanns, K., 2002. Characterization of laser-ablated and chemically reduced silver colloids in aqueous solution by UV/VIS spectroscopy and STM/SEM microscopy. Appl. Phys. B Lasers Opt. 75, 711–716.

Chauhan, R., Kumar, A., Abraham, J., 2013. Biological approach to the synthesis of silver nanoparticles with *Streptomyces* sp JAR1 and its antimicrobial activity. Sci. Pharm. 81 (2), 607–621.

Cochran, W.G., Snedecor, G.W., 1989. Statistical Methods. Iowa State University Press, Ames (IA), USA.

Deepa, S., Kanimozhi, K., Panneerselvam, A., 2013. Antimicrobial activity of extracellularly synthesized silver nanoparticles from marine derived actinomycetes. Int. J. Curr. Microbiol. Appl. Sci. 2 (9), 223–230.

Devika, R., Elumalai, S., Manikandan, E., Eswaramoorthy, D., 2012. Biosynthesis of silver nanoparticles using the fungus *Pleurotus osteatus* and their antimicrobial activity. Sci. Rep. 1, 557. http://dx.doi.org/10.4172/scientificreports.557.

El-Agamy, D., 2014. Microorganisms as Bionanofactories for Synthesis of Nanoparticles and their Applications. Ain Shams University, M.Sc. in biochemistry, Faculty of science.

El-Naggar, N.E., Abdelwahed, N.A.M., 2014. Application of statistical experimental design for optimization of silver nanoparticles biosynthesis by a nanofactory *Streptomyces viridochromogenes*. J. Microbiol. 52 (1), 53–63.

El-Sersy, N.A., Abdelwahab, A.E., Abouelkhir, S.S., Abou-Zeid, D., Sabry, S.A., 2012. Antibacterial and anticancer activity of e-poly-L-lysine (e-PL) produced by a marine *Bacillus subtilis* sp. J. Basic Microbiol. 52, 1–10.

Faghri, Zonooz.N., Salouti, M., 2011. Extracellular biosynthesis of silver nanoparticles using cell filtrate of *Streptomyces* sp. ERI-3. Sci. Iranica 18 (6), 1631–1635.

Fayaz, A.M., Balaji, K., Girilal, M., Yadav, R., Kalaichelvan, P.T., Venketesan, R., 2010. Biogenic synthesis of silver nanoparticles and their synergistic effect with antibiotics: a study against gram-positive and gram-negative bacteria. Nanomed. NBM 6, 103–109.

Golinska, P., Wypij, M., Ingle, A.P., Gupta, I., Dahm, H., Rai, M., 2014. Biogenic synthesis of metal nanoparticles from actinomycetes: biomedical applications and cytotoxicity. Appl. Microbiol. Biotechnol. 98 (19), 8083–8097.

Hall, T.A., 1999. BioEdit: a user-friendly biological sequence alignment editor and analysis program for Windows 95/98/NT. Nucl. Acids Symp. Ser. 4, 95–98.

Iravani, S., 2014. Bacteria in nanoparticle synthesis: current status and future prospects. Int. Scholarly Res. Not. 2014, 1–18.

Jaidev, L.R., Narasimha, G., 2010. Fungal mediated biosynthesis of silver nanoparticles, characterization and antimicrobial activity. Colloids Surf. B 8, 430–433.

Kaler, A., Jain, S., d Banerjee, U.C., 2013. Green and rapid synthesis of anticancerous silver nanoparticles by *Saccharomyces boulardii* and insight into mechanism of nanoparticle synthesis. BioMed Res. Int. 2013, 1–8.

Kamel, Z., Saleh, M., El Namoury, N., 2016. Biosynthesis, characterization, and antimicrobial activity of silver nanoparticles from actinomycetes. Res. J. Pharm. Biol. Chem. Sci. 7 (1), 119–127.

Kiran, G.S., Thomas, T.A., Selvin, J., Sabarathnam, B., Lipton, A.P., 2010. Optimization and characterization of a new lipopeptide biosurfactant produced by marine *Brevibacterium aureum* MSA13 in solid state culture. Bioresour. Technol. 101, 2389–2396.

Kumar, P.S., Balachandran, C., Duraipandiyan, V., Ramasamy, D., Ignacimuthu, S., Abdullah, Al.-Dhabi.N., 2015. Extracellular biosynthesis of silver nanoparticle using *Streptomyces* sp. 09 PBT 005 and its antibacterial and cytotoxic properties. Appl. Nanosci. 5, 169–180.

Kumaran, S., Radhakrishnan, M., Balagurunathan, R., 2011. Potential bioactive compound from marine actinomycetes against biofouling bacteria. J. Adv. Biotechnol. 10, 22–26.

Lakhsmi, S.Y.S., Lakhsmi, H., Sharmila, S., 2015. Isolation, screening, identification, characterization and applications of green synthesized silver nanoparticle from marine Actinomycetes-*streptomyces althioticus*. World J. Pharm. Res. 4 (7), 1592–1611.

Malarkodi, C., Rajeshkumar, S., Paulkumar, K., Gnanajobitha, G., Vanaja, M., Annadurai, G., 2013. Bacterial synthesis of silver nanoparticles by using optimized biomass growth of *Bacillus* sp. Nanosci. Nanotechnol. An Int. J. 3 (2), 26–32.

Mohamedin, A., El-Naggar, N.E., Hamza, S.S., Sherief, A.A., 2015. Green synthesis, characterization and antimicrobial activities of silver nanoparticles by *Streptomyces viridodiastaticus* SSHH-1 as a living nanofactory: statistical optimization of process variables. Curr. Nanosci. 11, 640–654.

Narasimha, G., Janardhan, Alzohairy, M., Khadri, H., Mallikarjuna, K., 2013. Extracellular synthesis, characterization and antibacterial activity of Silver nanoparticles by *Actinomycetes* isolative. Int. J. Nano Dimensions 4 (1), 77–83.

Prakasham, R.S., Kumar, B.S., Kumar, Y.S., Kumar, K.P., 2014. Production and characterization of protein encapsulated silver nanoparticles by marine isolate *Streptomyces parvulus* SSNP11. Indian J. Microbiol. 54 (3), 329–336.

Priyaragini, S., Sathishkumar, S.R., Bhaskararao, K.V., 2013. Biosynthesis of silver nanoparticles using actinobacteria and evaluating its antimicrobial and cytotoxicity activity. Int. J. Pharm. Pharm. Sci. 5 (2), 709–712.

Plackett, R.L., Burman, J.P., 1946. The design of optimum multi factorial experiments. Biometrica 33, 305–325.

Rai, M., Yadav, A., Gade, A., 2009. Silver nanoparticles as a new generation of antimicrobials. Biotechnol. Adv. 27, 76–83.

Ravikumar, S., Krishnakumar, S., 2010. Antagonistic activity of marine actinomycetes from Arabian Sea coast. Arch. Appl. Sci. Res. 2 (6), 273–280.

Reddy, G., Ramakrishna, D.P.N., Raja Gopal, S.V., 2011. A morphological, physiological and biochemical studies of marine *Streptomyces rochei* (MTCC 10,109) showing antagonistic activity against selective human pathogenic microorganisms. Asian J. Biol. Sci. 4 (1), 1–14.

Saminathan, K., 2015. Biosynthesis of silver nanoparticles using soil actinomycetes *Streptomyces* sp. Int. J. Curr. Microbiol. Appl. Sci. 4 (3), 1073–1083.

Samundeeswari, A., Priya Dhas, S., Nirmala, J., John, S.P., Mukherjee, A., Chandrasekaran, N., 2012. Biosynthesis of silver nanoparticles using actinobacterium *Streptomyces albogriseolus* and its antibacterial activity. Biotechnol. Appl. Biochem. 59 (6), 503–507.

Sastry, M., Ahmad, A., Khan, M.I., Kumar, R., 2003. Biosynthesis of metal nanoparticles using fungi and actinomycetes. Curr. Sci. 85, 162–170.

Sawada, I., Fachrul, R., Ito, T., Ohmukai, Y., Maruyama, T., Matsuyama, H., 2012. Development of a hydrophilic polymer membrane containing silver nanoparticles with both organic antifouling and antibacterial properties. J. Membr. Sci. 387, 1–6.

Selvakumar, P., Viveka, S., Prakash, S., Jasminebeaula, S., Uloganathan, R., 2012. Antimicrobial activity of extracellularly synthesized silver nanoparticles from marine derived *Streptomyces rochei*. Int. J. Pharm. Biol. Sci. 3 (3), 188–197.

Shaligram, N.S., Bule, M., Bhambure, R., Singhal, R.S., Singh, S.K., Szakacs, G., Pandey, A., 2009. Biosynthesis of silver nanoparticles using aqueous extract from the compactin producing fungal strain. Process Biochem. 44, 939–943.

Shawkey, A.M., Rabeh, M.A., Abdulall, A.K., Abdellatif, A.O., 2013. Green nanotechnology: anticancer activity of silver nanoparticles using *Citrullus colocynthis* aqueous extracts. Adv. Life Sci. Technol. 13, 60–70.

Shrivastava, S., Bera, T., Roy, A., Singh, G., Ramachandrarao, P., Dash, D., 2007. Characterization of enhanced antibacterial effects of novel silver nanoparticles. Nanotechnology 18, 9–12.

Singh, D., Rathod, V., Fatima, L., Kausar, A., Vidyashree, Anjum, N., Priyanka, B., 2014a. Biologically reduced silver nanoparticles from *Streptomyces* sp. VDP-5 and its antibacterial efficacy. Int. J. Pharm. Pharm. Sci. Res. 4 (2), 31–36.

Singh, D., Rathod, V., Ninganagouda, S., Hiremath, J., Kumar, A.S., Mathew, J., 2014b. Optimization and characterization of silver nanoparticle by endophytic fungi *Penicillium* sp. Isolated from Curcuma longa (Turmeric) and application studies against MDR *E. coli* and *S. aureus*. Bioinorg. Chem. Appl. 2014, 1–8. Article ID 408021.

Sosa, I.O., Noguez, C., Barrera, R.G., 2003. Optical properties of metal nanoparticles with arbitrary shapes. J. Phys. Chem. B 107, 6269–6275.

Yue, H., Chen, J., Sandvol, E., Ni, J., Hearn, T., Zhou, S., Feng, Y., Ge, Z., Trujillo, A., Wang, Y., Jin, G., Jiang, M., Tang, Y., Liang, X., Wei, S., Wang, H., Fan, W., 2012. Lithospheric and upper mantle structure of the northeastern Tibetan plateau. J. Geophys. Res. 117, 1–18.

Zarina, A., Nanda, A., 2014a. Combined efficacy of antibiotics and biosynthesised silver nanoparticles from *Streptomyces albaduncus*. Int. J. Pharm. Technol. Res. 6 (6), 1862–1869.

Zarina, A., Nanda, A., 2014b. Green approach for synthesis of silver nanoparticles from marine *Streptomyces*- MS 26 and their antibiotic efficacy. J. Pharm. Sci. Res. 6 (10), 321–327.

Zayed, M.F., Eisa, W.H., Shabaka, A.A., 2012. *Malva parviflora* extract assisted green synthesis of silver nanoparticles. Spectrochim. Acta Part A Mol. Biomol. Spectrosc. 98 (1), 423–428.